

The *in vitro* manipulation of carbohydrate metabolism: a new strategy for deciphering the cellular defence mechanisms against nitric oxide attack

Claire LE GOFFE, Geneviève VALLETTE, Anne JARRY, Chantal BOU-HANNA and Christian L. LABOISSE¹

INSERM CJF 94-04, Faculté de Médecine, 1 rue Gaston Veil, 44035 Nantes, France

This study was aimed at examining the effects of manipulating the carbohydrate source of the culture medium on the cellular sensitivity of epithelial cells to an oxidative attack. Our rationale was that substituting galactose for glucose in culture media would remove the protection afforded by glucose utilization in two major metabolic pathways, i.e. anaerobic glycolysis and/or the pentose phosphate pathway (PPP), which builds up cellular reducing power. Indeed, we show that the polarized human colonic epithelial cell line HT29-Cl.16E was sensitive to the deleterious effects of the NO donor PAPANONOate [3-(2-hydroxy-2-nitroso-1-propylhydrazino)-1-propanamine] only in galactose-containing medium. In such medium NO attack led to cytotoxic and apoptotic cell death, associated with formation of derivatives of NO auto-oxidation (collectively termed NO_x) and peroxynitrite, leading to intracellular GSH depletion and nitrotyrosine formation. The addition of 2-deoxyglucose, a non-

glycolytic substrate, to galactose-fed cells protected HT29-Cl.16E cells from NO attack and maintained control GSH levels through its metabolic utilization in the PPP, as shown by ¹⁴CO₂ production from 2-deoxy[1-¹⁴C]glucose. Therefore, increasing the availability of reducing equivalents without interfering with energy metabolism is able to prevent NO-induced cell injury. Finally, this background provides the conceptual framework for establishing nutritional manipulation of cellular metabolic pathways that could provide new means for (i) deciphering the mechanisms of cell injury by reactive nitrogen species and reactive oxygen species at the whole-cell level and (ii) establishing the hierarchy of intracellular defence mechanisms against these attacks.

Key words: apoptosis, cytotoxicity, human epithelial cell, reactive nitrogen species, reducing power.

INTRODUCTION

The so-called barrier epithelia (epidermis, tracheobronchial epithelia and intestinal epithelia for example) are subjected to a variety of aggressions, including attacks by reactive oxygen (ROS) and reactive nitrogen species (RNOS) [1,2]. The overwhelming of the cellular defence mechanisms by overproduction of ROS or RNOS is thought to play a pivotal role in the breakdown of the epithelial barrier during an inflammatory reaction. Surprisingly, primary cultures of epithelial cells or epithelial cell lines are highly resistant to a variety of oxidant challenges [3–7]. Nutritional conditions met by cells maintained in standard media, containing high concentrations of glucose (up to 25 mM in Dulbecco's modified Eagle's medium, DMEM), could strengthen their defence against an oxidative attack. Indeed, glucose builds up the cellular reducing power via its metabolism by the pentose phosphate pathway (PPP) [8]. In addition, high glucose concentrations force the cells to draw their energy from anaerobic glycolysis (the Crabtree effect) [9], a metabolic pathway that secures ATP production even under conditions that cause mitochondrial dysfunction. Finally, lactate and pyruvate generated by anaerobic glycolysis are known to act as ROS scavengers [10–12]. Substituting galactose for glucose in culture media is known to alter the cellular energy metabolism in various normal cell types without modifying their growth rates [13]. In galactose medium, very little lactate and pyruvate accumulate in the medium because of the restricted flow of galactose to glucose 6-phosphate. The mode of metabolism is therefore one in which very little ATP synthesis derives from glycolysis, the majority being derived from mitochondrial oxidation of pyruvate [13]. In fact, a galactose-containing medium

offers several theoretical advantages for studying the cellular responses to an endogenous or exogenous oxidative attack. First, in these culture conditions ATP production relies on mitochondrial functional integrity. In addition, functioning mitochondria are likely to generate ROS via their respiratory chain, this reaction being potentially important in mounting a cellular stress [10,14–16]. Second, pyruvate consumption in the tricarboxylic acid cycle deprives the cells of ROS-scavenging species, i.e. lactate and pyruvate [13]. Finally, the restricted flow of galactose to glucose 6-phosphate may prevent the build up of a reducing power upon PPP stimulation by an oxidant attack.

In this work, we set up an experimental system *in vitro*, in which a burst of RNOS was applied via the NO donor PAPANONOate [3-(2-hydroxy-2-nitroso-1-propylhydrazino)-1-propanamine] to a differentiated human colonic epithelial cell line (HT29-Cl.16E) maintained in two distinct sets of culture conditions differing in the nature of the carbohydrate source. Here we show for the first time that changing the carbohydrate source allows the control of an oxidant stress through the manipulation of the ways in which the cells produce their ATP and their reducing power. Finally, our findings show that it is of the utmost importance to monitor the ways in which the cells utilize their carbohydrate source when it comes to unravelling the deleterious effects of an oxidative stress.

MATERIALS AND METHODS

Cell culture and treatment

The HT29-Cl.16E cell line [17], a well-characterized [18–20] polarized human colonic epithelial cell line, was routinely grown

Abbreviations used: DMEM, Dulbecco's modified Eagle's medium; LDH, lactate dehydrogenase; ONOO⁻, peroxynitrite; PPP, pentose phosphate pathway; RNOS, reactive nitrogen species; ROS, reactive oxygen species; PAPANONOate, 3-(2-hydroxy-2-nitroso-1-propylhydrazino)-1-propanamine; GSNO, nitrosogluthathione; FCS, fetal calf serum; NO_x, derivatives of NO auto-oxidation.

¹ To whom correspondence should be addressed (e-mail laboisce@sante.univ-nantes.fr).

in DMEM/10% (v/v) fetal calf serum (FCS; both from Life Technologies).

For the experiments, HT29-Cl.16E cells were seeded at 250 000 cells/well in six-well multi-well culture plates (Costar) and maintained for 48 h in DMEM/10% FCS. The medium was replaced with either DMEM/25 mM glucose/10% dialysed FCS (glc-DMEM) or DMEM without glucose (Life Technologies) supplemented with 5 mM galactose/10% dialysed FCS (gal-DMEM) 24 h before the experiments. At time point zero of the experiments, the medium was changed and PAPANONOate (Cayman Chemicals) was added at the concentrations indicated and incubated for various periods of time as mentioned in the Figure legends.

Characterization and quantification of cell death

Cell death was quantified using different procedures. Cell counting was performed using a haemocytometer chamber. Cytotoxicity was determined by lactate dehydrogenase (LDH) release using an Enzyline LDH Kit (Biomerieux). Apoptosis was determined by staining of nuclei with the DNA-specific dye Hoechst 33258 (0.5 µg/ml; Calbiochem) on cytospin preparations of cells.

Measurement of intracellular ATP

Cells were treated with ice-cold 12% (v/v) trichloroacetic acid solution to eliminate proteins. After centrifugation (800 g, 10 min), aliquots of cellular extract were assayed for ATP content using an enzymic determination coupling the phosphorylation of 3-phosphate glycerate by ATP to the dephosphorylation catalysed by glycerate-phosphate dehydrogenase that involves the oxidation of NADH [21]. Formation of NAD was quantified by monitoring the decrease in absorbance at 340 nm. The protein pellet was solubilized in 1 M NaOH and protein assay was performed using the Bradford method (Bio-Rad). ATP concentrations were expressed as nmol/mg of protein.

Measurement of lactate and pyruvate accumulation

Aliquots of deproteinized medium were assayed for lactate and pyruvate using the lactate dehydrogenase enzymic procedure [22]. The amount of pyruvate was measured by monitoring at 340 nm the oxidation of NADH to NAD⁺. For lactate assay the equilibrium of the reaction was displaced in favour of pyruvate and NADH formation by glutamate-pyruvate transaminase in the presence of glutamate. NADH formation was monitored at 340 nm and was proportional to lactate concentration.

Determination of intracellular GSH content

Cells were harvested by scraping into PBS with a 'rubber policeman', and sonicated at 0 °C. The cell homogenate was centrifuged (12 000 g, 10 min) and the supernatant incubated for 5 min at room temperature with 10% metaphosphoric acid (v/v). The mixture was centrifuged (15 000 g, 5 min) and the supernatant analysed for GSH and GSSG content by the GSH disulphide reductase 5,5'-dithiobis (2-nitrobenzoic acid) recycling method using the procedure described in the glutathione assay kit from Cayman Chemicals [23,24]. The protein pellet was solubilized in 1 M NaOH and protein assay was performed using the Bradford method (Bio-Rad). Results were determined as nmol of GSH/mg of protein and expressed as the percentage intracellular GSH or GSSG of total glutathione (GSSG + GSH).

Determination of 3-nitrotyrosine

The 3-nitrotyrosine quantification was performed on cellular lysates with a newly designed ELISA (TCS Biological nitrotyrosine ELISA kit). In this assay the microplate was precoated with a predetermined amount of nitrated proteins. A standard curve was constructed using serial dilutions of nitrated BSA, which competed with immobilized nitrated proteins for the polyclonal anti-nitrotyrosine antibody. Protein assay was measured in the cell lysates using Folin's method (Bio-Rad). Results are expressed as µg of 'nitrated BSA equivalent'/mg of protein.

Characterization of nitrosogluthione (GSNO) formation

GSNO formation was monitored spectrophotometrically at 340 nm in quartz cuvettes [25,26]. Anaerobic samples were prepared from de-aerated medium and all the operations were performed within a nitrogen atmosphere using a glove box. After sealing, the cuvettes were incubated at 37 °C and transferred to the spectrophotometer (Perkin-Elmer) for monitoring absorbance at 340 nm every 10 min up to 2.5 h. GSNO concentrations were calculated from a GSNO standard curve (0–1 mM) and were expressed as µM GSNO.

¹⁴CO₂ production from 2-deoxy[1-¹⁴C]glucose

HT29-Cl.16E cells were treated or not with 10⁻³ M PAPANONOate and assayed for ¹⁴CO₂ production over various periods of time by adding 0.2 µCi/ml 2-deoxy[1-¹⁴C]glucose (specific radioactivity 57 mCi/mmol) to gal-DMEM medium supplemented with 100 µM 2-deoxyglucose. Cellular metabolism was stopped by adding perchloric acid. Hydroxyhyamine (Sigma) was used to capture the ¹⁴CO₂ produced, as described previously [27], and radioactivity was measured via liquid scintillation counting (Packard Tri-Carb 2100 TR). Assessment of CO₂ recovery (95 ± 6%, mean ± S.E.M.) was performed by adding 0.125 µCi of NaH¹⁴CO₃ to separate wells. Results were expressed as nmol of CO₂/mg of protein.

RESULTS AND DISCUSSION

Several lines of investigation have shown that oxidative stresses including RNOS-induced cell death involve disruption of GSH homeostasis [28–30], mitochondrial dysfunction [15,31] and impairment of ATP production ([32–34], for a review see [35]). However, deciphering the hierarchy of these events has remained a difficult task. In addition, recent studies point to NO as a mediator able to shift apoptotic cell death towards necrosis via lowering intracellular ATP [36].

As a first step towards understanding the mechanisms of RNOS-induced oxidative stress, we set up culture conditions allowing the cells to draw their energy from glycolysis, i.e. high-glucose (25 mM) medium (glc-DMEM), or from oxidative phosphorylations, i.e. galactose medium (gal-DMEM). HT29-Cl.16E cells grew equally well in both media, as do several normal cell types [13]. However, cells deficient in mitochondrial functions [13] as well as some undifferentiated cancer cells [37] are unable to grow in gal-DMEM.

Exposure of exponentially growing HT29-Cl.16E cells maintained in high-glucose (25 mM) medium to increasing concentrations of oligomycin, an F₁/F₀ ATPase inhibitor, did not impair cell viability (Figure 1A) or cellular ATP content (Figure 1B). In addition, our observations of lactate and pyruvate accumulation in the culture media provide further experimental evidence for the glycolytic degradation of glucose into lactate and pyruvate in these culture conditions (Table 1). In contrast,

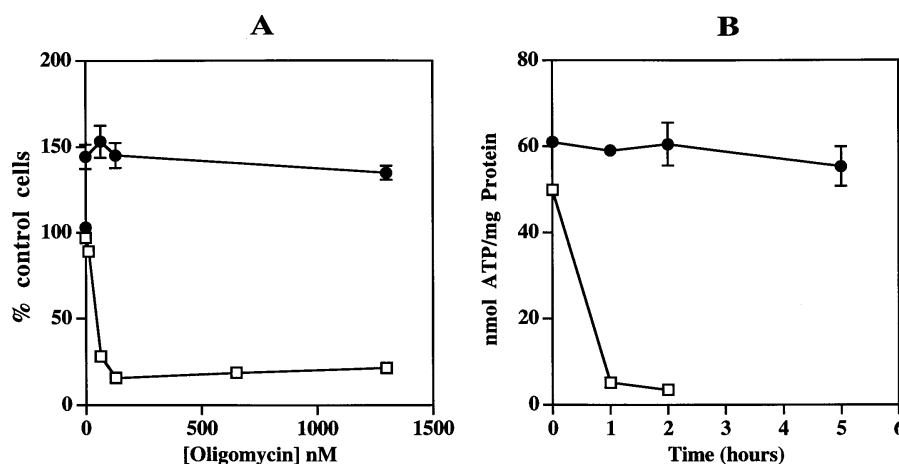


Figure 1 Oligomycin effect on cell viability and intracellular ATP level of HT-29Cl.16E cells cultured in gal-DMEM or glc-DMEM

(A) HT29-Cl.16E cells cultured in either glc-DMEM (●) or gal-DMEM (□) were incubated for 24 h with increasing concentrations of oligomycin. Cell viability was determined by counting adherent cells after treatment and results are expressed as a percentage of control cells. (B) HT29-Cl.16E cells were cultured in either glc-DMEM (●) or gal-DMEM (□) in the presence of 1.3 μ M oligomycin. ATP was measured at various time points as described in the Materials and methods section and results are expressed as nmol of ATP/mg of protein. Each point represents the mean \pm S.E.M. of 3–7 determinations. Data points without error bars indicate S.E.M. values less than the symbol size.

Table 1 Pyruvate and lactate accumulation in glc- or gal-DMEM culture media

Lactate and pyruvate accumulation was measured in the culture media of HT29-Cl.16E cells grown for 24 h in glc-DMEM or gal-DMEM, with or without 5 mM 2-deoxyglucose. Each value represents the mean \pm S.E.M. of 3 determinations.

Culture medium	Pyruvate (mM)	Lactate (mM)
Glc-DMEM	0.28 \pm 0.01	8.5 \pm 0.4
Gal-DMEM	0.033 \pm 0.004	0.33 \pm 0.03
Gal-DMEM + 2-deoxyglucose	0.028 \pm 0.003	0.36 \pm 0.04

when glucose was replaced by galactose, exposure to oligomycin led to a dose-dependent cytotoxic effect (Figure 1A) that was associated with cellular ATP depletion (Figure 1B), with as little as 1 h of incubation. These findings, together with our observation of the absence of lactate and pyruvate accumulation in the culture media (Table 1), are in line with the concept that in galactose-containing medium the cells draw their energy from oxidative phosphorylations.

To study the effects of RNOS, HT29-Cl.16E cells cultured in either glc-DMEM or gal-DMEM were exposed to the NO donor PAPANONOate. Treatment of HT29-Cl.16E cells cultured in glc-DMEM with increasing concentrations of PAPANONOate did not impair cell viability (Figure 2). In contrast, PAPANONOate exerted a dose-dependent cytotoxic effect towards HT29-Cl.16E cells cultured in gal-DMEM, with a maximal effect at 10^{-3} M (Figure 2). This effect was abolished by oxyhaemoglobin, which binds NO. The nature of the deleterious effects of NO on gal-DMEM HT29-Cl.16E cells as well as the time course of these events were monitored at 10^{-3} M PAPANONOate. As shown in Figure 3(A), NO provoked a massive cellular detachment as early as 5 h, associated with cellular apoptosis (Figure 3B) and cellular necrosis (Figure 3C). At 5 h, nearly 75% of the cells were detached and nearly 40% of the detached cells underwent apoptosis, as shown by Hoechst

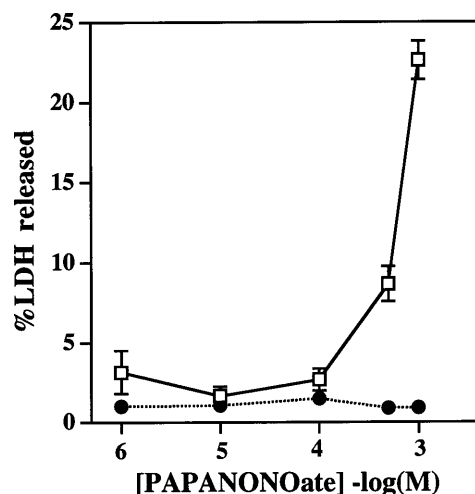


Figure 2 Dose-dependent effects of RNOS on the viability of HT29-Cl.16E cells cultured in gal-DMEM or glc-DMEM

HT29-Cl.16E cells cultured in either glc-DMEM (●) or gal-DMEM (□) were incubated for 14 h in the presence of increasing doses of PAPANONOate. Cytotoxicity was determined by measuring the LDH released in the culture medium. Each point represents the mean \pm S.E.M. of 3 determinations. Data points without error bars indicate S.E.M. values less than the symbol size.

staining of nuclei on cytocentrifuged preparations (Figure 3B). Cell detachment was preceded by a 50% fall in intracellular ATP after a 2 h incubation with PAPANONOate.

To gain more insight into the mechanisms which translate RNOS production into apoptotic and cytotoxic cell death, we then measured intracellular GSH and GSSG contents in gal-DMEM-grown, PAPANONOate-treated, HT29-Cl.16E cells. As shown in Figure 4(A), PAPANONOate (10^{-3} M) induced a GSH

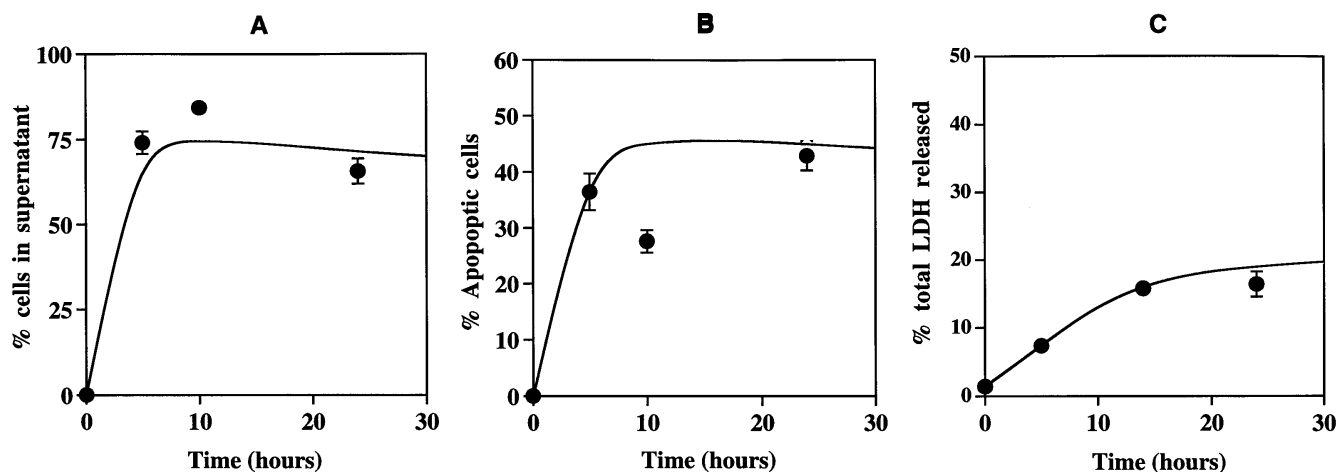


Figure 3 Time course of RNOS effects on HT29-Cl.16E cells viability

HT29-Cl.16E cells cultured in gal-DMEM were incubated with 10^{-3} M PAPANONOate. (A) Cell detachment was determined by counting adherent cells and cells in suspension. Results are expressed as the percentage of cells in the supernatant over total cells. (B) Cytospin preparations of cells in suspension were stained by Hoechst 33258. Apoptotic cells were counted under a fluorescence microscope and results are expressed as the percentage apoptotic cells of total cells in the supernatant. (C) Cytotoxicity was determined by measuring LDH released into the culture medium. Each point represents the mean \pm S.E.M. of 3 determinations. Data points without error bars indicate S.E.M. values less than the symbol size.

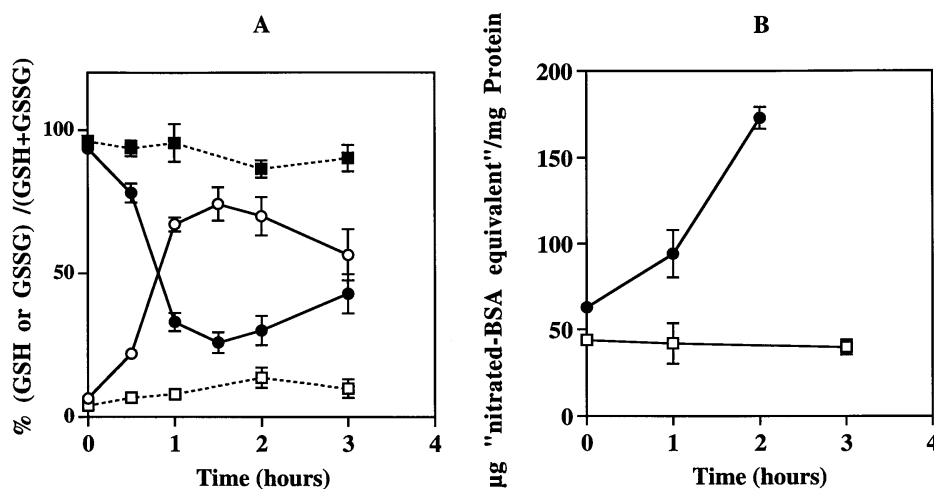


Figure 4 Time course of RNOS effects on intracellular GSH and 3-nitrotyrosine levels: effect of 2-deoxyglucose treatment

HT29-Cl.16E cells cultured in gal-DMEM with (\square , \blacksquare) or without (\circ , \bullet) 5 mM 2-deoxyglucose were treated for various periods of time with 10^{-3} M PAPANONOate. (A) Intracellular GSH and GSSG were measured as described in the Materials and methods section. Results are expressed as the percentage of GSH (\bullet , \blacksquare) or GSSG (\circ , \square) over total glutathione (GSH + GSSG). (B) 3-Nitrotyrosine level in the presence (\square) or absence (\bullet) of 2-deoxyglucose was measured by an ELISA method as described in the Materials and methods section. Results are expressed as μ g of 'nitrated BSA equivalent'/mg of protein. Each point represents the mean \pm S.E.M. of 3–4 determinations. Data points without error bars indicate S.E.M. values less than the symbol size.

depletion as early as 1 h, associated with a concomitant increase of GSSG.

At this point of the exploitation of our experimental system, it was important to determine the nature of the RNOS involved in the GSH depletion. There are two likely candidates for depleting GSH content at high NO concentrations: (i) derivatives of NO auto-oxidation, collectively termed NOx, which are scavenged by GSH leading to GSNO; and (ii) ONOO⁻ (peroxynitrite) resulting from the reaction of NO with superoxide ions (O₂⁻), leading to GSH oxidation [38]. In fact, functioning mitochondria are likely to generate O₂⁻ upon inhibition by NO of electron transfer [14–16]. To examine whether NOx were formed in our experimental conditions, we monitored GSNO formation

spectrophotometrically at 340 nm in the presence of 1 mM GSH in a cell-free culture medium. As shown in Figure 5, addition of PAPANONOate (1 mM) in aerobic conditions induced a rapid and stable increase in absorbance at 340 nm, reflecting the formation of GSNO. Addition of Hg²⁺ led to an abrupt fall in absorbance, indicating the breakdown of GSNO. Anaerobically, almost no GSNO was formed. We next measured the extent of protein tyrosine nitration using an ELISA for 3-nitrotyrosine determination. As shown in Figure 4(B), we observed a rapid and significant increase in tyrosine nitration, which paralleled GSH depletion. With ONOO⁻ being the most likely RNOS to form nitrotyrosine [39], it is then collectively concluded that two RNOS are involved in the GSH depletion, NOx and ONOO⁻. As

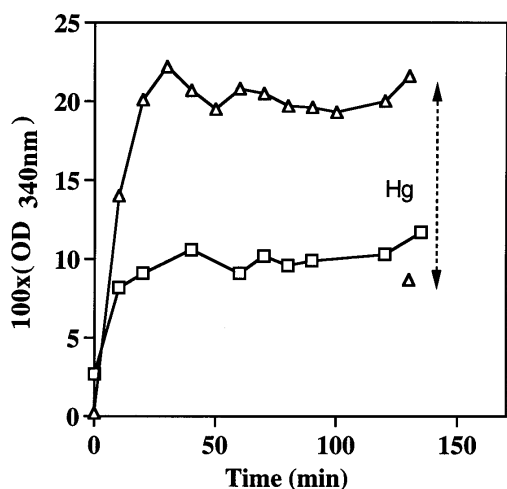


Figure 5 GSN0 formation from co-incubation of GSH and PAPANONOate

GSH (1 mM) was incubated with 1 mM PAPANONOate in DMEM without Phenol Red in a spectrophotometer cuvette at 37 °C under aerobic (Δ) and anaerobic (\square) conditions. GSN0 formation was monitored by following the absorbance (OD) at 340 nm every 10 min for 2.5 h, and 0.1% HgCl_2 was added at time point 130 min (Δ). The calculated GSN0 concentration at 130 min was 126 μM .

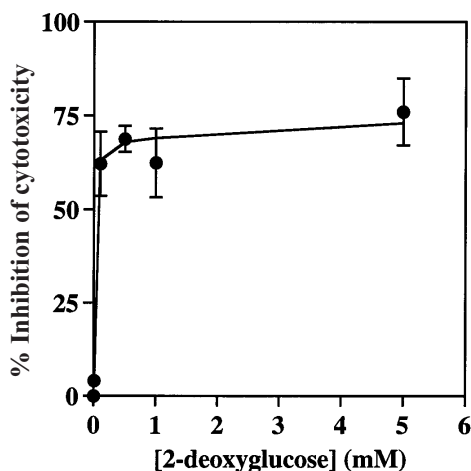


Figure 6 Protective effect of 2-deoxyglucose on RNOS-induced cytotoxicity in HT29-Cl.16E cells

HT29-Cl.16E cells maintained in gal-DMEM were treated for 14 h with 10^{-3} M PAPANONOate in the presence of increasing doses of 2-deoxyglucose. Cytotoxicity was determined by measuring LDH released in the culture medium. Results are expressed as the percentage inhibition of cytotoxicity by 2-deoxyglucose over the control. Each point represents the mean \pm S.E.M. of 3–6 determinations. Data points without error bars indicate S.E.M. values less than the symbol size.

to whether ONOO^- formation in gal-DMEM is a consequence of mitochondrial dysfunction upon exposure to NO is under investigation in our laboratory.

The next step of this study was to try to relieve gal-DMEM-cultured HT29-Cl.16E cells from NO attack. Based on our observation of GSH depletion upon PAPANONOate treatment, we reasoned that increasing the availability of the PPP substrate, i.e. glucose 6-phosphate, could help regenerate GSH via NADPH recycling. To selectively feed the PPP without interfering with the energy metabolism pathway, 2-deoxyglucose was added to the

Table 2 CO_2 production from 2-deoxy[1- ^{14}C]glucose in HT29-Cl.16E cells cultured in gal-DMEM

$^{14}\text{CO}_2$ Production from 2-deoxy[1- ^{14}C]glucose was measured as described in the Materials and methods. Each value represents the mean \pm S.E.M. of 6–9 determinations. * $P < 0.013$ versus control; ** $P < 0.001$ versus control (Student's t test).

Time of incubation	$^{14}\text{CO}_2$ Production (nmol of CO_2 /mg of protein)	
	Control	10^{-3} M PAPANONOate
1 h	11.25 ± 2.68	$22.26 \pm 3.09^*$
2 h	17.84 ± 2.26	$73.71 \pm 7.46^{**}$

culture medium. We hypothesized that 2-deoxyglucose can enter the PPP after its phosphorylation into 2-deoxyglucose 6-phosphate [40] and support NADPH recycling [41] without interfering with the glycolytic utilization of galactose due to the existence of two distinct pathways of phosphorylation of galactose and glucose on C-6. Therefore, it follows that adding 2-deoxyglucose to galactose-fed cells would strengthen the PPP without interfering with the energy metabolism. Indeed, as shown in Figure 6, the addition of 2-deoxyglucose to galactose-fed, NO-treated, cells led to a dose-dependent protection of the cultured cells without altering the glycolytic utilization of galactose (Table 1). Preincubation of the cells with 6-deoxyglucose, a compound that enters the cells but is not phosphorylated [42], never exerted protective effects against RNOS, a finding showing that the protective effect depends on the conversion of 2-deoxyglucose into 2-deoxyglucose 6-phosphate. To further examine the mechanisms accounting for the protection by 2-deoxyglucose, we measured (i) $^{14}\text{CO}_2$ production from 2-deoxy[1- ^{14}C]glucose and (ii) intracellular GSH levels, which are linked directly to NADPH recycling. PAPANONOate (10^{-3} M) time-dependently stimulated $^{14}\text{CO}_2$ production (Table 2), showing that 2-deoxyglucose is metabolized in the oxidative branch of the PPP. This finding supports the concept that NO-induced cytotoxicity was due to a restricted flow of galactose to the PPP, thus preventing the build-up of a suitable level of reducing power. As expected from an agent that is able to regenerate NADPH via the PPP, 2-deoxyglucose prevented GSH depletion and maintained GSH homeostasis (Figure 4A). In addition, the restoration of GSH homeostasis by 2-deoxyglucose protected against tyrosine nitration (Figure 4B), a finding in line with the demonstration by Whiteman and Halliwell [43] that GSH is able to prevent peroxynitrite-mediated tyrosine nitration.

Several conclusions can be drawn from these findings. First, replacing glucose with galactose in culture media leads to loss of major cellular protective mechanisms against oxidative stress, e.g. the cell capacity to build up a reducing power and to generate metabolites acting as radical scavengers. Second, this loss of protective mechanisms is illustrated in our experiments by the cytotoxic and apoptotic effects of RNOS in galactose-fed cells. Third, we show in this work that increasing the availability of reducing equivalents without interfering with energy metabolism is able to prevent NO-induced cell injury. Finally, this background provides the conceptual framework for establishing nutritional manipulation of cells that could theoretically provide new means for (i) deciphering the mechanisms of cell injury by ROS and RNOS and (ii) establishing the hierarchy of intracellular defence mechanisms against these attacks.

We thank Myriam Robard for excellent technical assistance. This study was supported by the Conseil Départemental de Loire Atlantique de la Ligue Nationale Contre le Cancer, the Conseil Régional des Pays de Loire and the Association Française de Lutte contre la Mucoviscidose (AFLM).

REFERENCES

- 1 McKenzie, S. J., Baker, M. S., Buffinton, G. D. and Doe, W. F. (1996) *J. Clin. Invest.* **98**, 136–141
- 2 Alican, I. and Kubes, P. (1996) *Am. J. Physiol.* **270**, G225–G237
- 3 Becquet, F., Courtois, Y. and Goureau, O. (1994) *J. Cell. Physiol.* **159**, 256–262
- 4 Kubes, P., Reinhardt, P. H., Payne, D. and Woodman, R. C. (1995) *Am. J. Physiol.* **32**, G34–G41
- 5 Salzman, A. L., Menconi, M. J., Unno, N., Ezzel, R. M., Casey, D. M., Gonzales, P. K. and Fink, M. P. (1995) *Am. J. Physiol.* **268**, G361–G373
- 6 DuVall, M. D., Guo, Y. and Matalon, S. (1998) *Am. J. Physiol.* **275**, C1313–C1322
- 7 Vallette, G., Tenaud, I., Branka, J.-E., Jarry, A., Sainte-Marie, I., Dreno, B. and Laboisse, C. L. (1998) *Biochem. J.* **331**, 713–717
- 8 Aw, T. Y. and Rhoads, C. A. (1994) *J. Clin. Invest.* **94**, 2426–2434
- 9 McKay, N., Robinson, B., Brodie, R. and Rook-Allen, N. (1983) *Biochim. Biophys. Acta* **762**, 198–204
- 10 Brand, K. A. and Hermfisse, U. (1997) *FASEB J.* **11**, 388–395
- 11 Desagher, S., Glowinski, J. and Prémont, J. (1997) *J. Neurosci.* **17**, 9060–9067
- 12 Herz, H., Blake, D. R. and Grootveld, M. (1997) *Free Radicals Res.* **26**, 19–35
- 13 Robinson, B. H. (1996) *Methods Enzymol.* **264**, 454–464
- 14 Cassina, A. and Radi, R. (1996) *Arch. Biochem. Biophys.* **328**, 309–316
- 15 Lizasoain, I., Moro, M. A., Knowles, R. G., Darley-Usmar, V. and Moncada, S. (1996) *Biochem. J.* **314**, 877–880
- 16 Podesoro, J. J., Carreras, M. C., Lisdero, C., Riobo, N., Schoper, F. and Boderis, A. (1996) *Arch. Biochem. Biophys.* **328**, 85–92
- 17 Augeron, C. and Laboisse, C. L. (1984) *Cancer Res.* **44**, 3961–3969
- 18 Merlin, D., Augeron, C., Tien, X.-Y., Guo, X., Laboisse, C. L. and Hopfer, U. (1994) *J. Membr. Biol.* **137**, 137–149
- 19 Jarry, A., Merlin, D., Hopfer, U. and Laboisse, C. L. (1994) *Biochem. J.* **304**, 675–678
- 20 Guo, X. W., Merlin, D., Laboisse, C. and Hopfer, U. (1997) *Am. J. Physiol.* **273**, C804–C809
- 21 Adams, H. (1963) in *Methods of Enzymatic Analysis* (Bergmeyer, H. U., ed.), pp. 539–543, Academic Press, New York
- 22 Fleischer, W. R. (1970) in *Standard Methods in Clinical Chemistry*, vol. 6 (MacDonald, R. P., ed.), pp. 245–259, Academic Press, New York
- 23 Tietze, F. (1969) *Anal. Biochem.* **27**, 502–522
- 24 Griffith, O. W. (1980) *Anal. Biochem.* **106**, 2107–2121
- 25 Stamler, J. S. and Feelish, M. (1996) in *Methods in Nitric Oxide Research* (Feelish, M. and Stamler, J. S., eds.), pp. 522–539, John Wiley & Sons, Chichester
- 26 Hogg, N., Singh, R. J. and Kalyanaraman, B. (1996) *FEBS Lett.* **382**, 223–228
- 27 Bartos, D., Vlessis, A. A., Muller, P., Mela-Riker, L. and Trunkey, D. D. (1993) *Anal. Biochem.* **213**, 241–244
- 28 Luperchio, S., Tamir, S. and Tannenbaum, S. R. (1996) *Free Radical Biol. Med.* **21**, 513–519
- 29 Wakulich, C. A. and Tepperman, B. L. (1997) *Eur. J. Pharmacol.* **319**, 333–341
- 30 Hotherhall, J. S., Cunha, F. Q., Neild, G. H. and Noronha-Dutra, A. A. (1997) *Biochem. J.* **322**, 477–481
- 31 Clementi, E., Brown, G. C., Felisch, M. and Moncada, S. (1998) *Proc. Natl. Acad. Sci. U.S.A.* **95**, 7631–7636
- 32 Salzman, A. L., Menconi, M. J., Unno, N., Ezzel, R. M., Casey, D. M., Gonzalez, P. K. and Fink, M. P. (1995) *Am. J. Physiol.* **268**, G361–G373
- 33 Brorson, J. R., Schumacker, P. T. and Zhang, H. (1999) *J. Neurosci.* **19**, 147–158
- 34 Pieper, A. A., Verma, A., Zhang, J. and Snyder, S. H. (1999) *Trends Pharmacol. Sci.* **20**, 171–181
- 35 Kehrer, J. P. and Lund, L. G. (1994) *Free Radical Biol. Med.* **17**, 65–75
- 36 Leist, M., Single, B., Naumann, H., Fava, E., Simon, B., Kuhnle, S. and Nicotera, P. (1999) *Exp. Cell. Res.* **249**, 396–403
- 37 Pinto, M., Appay, M. D., Simon-Assman, P., Chevalier, G., Dracopoli, N., Fogh, J. and Zweibbaum, A. (1982) *Biol. Cell* **44**, 193–196
- 38 Wink, D. A., Grisham, M. B., Mitchell, J. B. and Ford, P. C. (1996) *Methods Enzymol.* **268**, 12–31
- 39 Beckman, J. S. and Koppenol, W. H. (1996) *Am. J. Physiol.* **271**, C1424–C1437
- 40 Rist, R. J., Jones, G. E. and Naftalin, R. J. (1990) *Biochem. J.* **265**, 243–249
- 41 Suzuki, M., O'Dea, J. D., Suzuki, T. and Agar, N. S. (1983) *Comp. Biochem. Physiol. B* **75**, 195–197
- 42 Romano, A. H. and Connell, N. D. (1982) *J. Cell Physiol.* **111**, 77–82
- 43 Whiteman, M. and Halliwell, B. (1996) *Free Radical Res.* **25**, 275–283

Received 23 July 1999/20 September 1999; accepted 11 October 1999